Photodissociation dynamics of the methyl perthiyl radical at 248 nm via photofragment translational spectroscopy

Neil C. Cole-Filipiak, Bogdan Negru, Gabriel M. P. Just,[a] Dayoung Park, and Daniel M. Neumark[b]

Department of Chemistry, University of California, Berkeley, Berkeley, California 94720, USA and Chemical Sciences Division, Lawrence Berkeley National Laboratory, Berkeley, California 94720, USA

(Received 2 November 2012; accepted 14 January 2013; published online 1 February 2013)

Photofragment translational spectroscopy was used to study the photodissociation of the methyl perthiyl radical CH_3SS at 248 nm. The radical was produced by flash pyrolysis of dimethyl disulfide (CH_3SSCH_3). Two channels were observed: $CH_3 + S_2$ and $CH_2S + SH$. Photofragment translational energy distributions indicate that $CH_3 + S_2$ results from C–S bond fission on the ground state surface. The $CH_2S + SH$ channel can proceed through isomerization to CH_2SSH on the ground state surface but also may involve production of electronically excited CH_2S. © *2013 American Institute of Physics*. [http://dx.doi.org/10.1063/1.4789485]

I. INTRODUCTION

The disulfide bond plays a key role in diverse areas of chemistry ranging from chemical biology, where it plays a critical role in protein folding and structure as the cysteine bond,[1] to atmospheric chemistry, where it is found in atmospherically relevant species that take part in the sulfur cycle.[2] These considerations have motivated fundamental studies of the gas-phase chemistry and photochemistry of alkyl disulfides, with dimethyl disulfide (DMDS) at the forefront of many investigations.[3–17] Depending on the wavelength used, the competing dissociation pathways for DMDS are as follows:[15]

$$CH_3SSCH_3 + h\nu \rightarrow 2CH_3S\,(\tilde{X}^2E) \quad \Delta H_o = 70\,\text{kcal/mol}, \tag{1}$$

$$CH_3SSCH_3 + h\nu \rightarrow CH_3SS\,(\tilde{X}^2A'') + CH_3\,(\tilde{X}^2A_2'') \quad \Delta H_o = 55\,\text{kcal/mol}. \tag{2}$$

Channel (2) has been of special interest due to the CH_3SS (methyl perthiyl) radical produced. Callear and Dickson studied this pathway at ca. 195 nm, and observed CH_3 and S_2 photoproducts.[4] Pressure dependence studies for this channel demonstrated that internally excited CH_3SS from channel (2) decayed spontaneously to produce the S_2 fragment. Subsequently, Ng and co-workers[14] observed both the methyl perthiyl radical and S_2 fragments from the 193 nm photodissociation of DMDS and attributed the S_2 signal to absorption of a second photon rather than a secondary process. Additional studies at 193 nm by Lee *et al.*[15] and Martínez-Haya *et al.*[16] showed that spontaneous decay of hot CH_3SS was the primary source of S_2, but that there was a smaller contribution from photoexcitation of CH_3SS. Kumar *et al.*[18] studied the 248 nm photodissociation of DMDS via transient absorption spectroscopy in a static cell. They reported several UV absorption bands that they assigned to CH_3S and S_2 photofragments. The more recent work by Lee *et al.*[15] showed that the collisionless photodissociation of DMDS at 248 nm exclusively occurs via channel (1). They attributed the exclusivity to a $\sigma_{ss}^* \leftarrow n_s$ electronic excitation, resulting in a rapid, bond-specific dissociation.

In this work, we investigate the photodissociation of the methyl perthiyl radical itself at 248 nm. Several experimental and theoretical studies of CH_3SS have been reported previously. Moran and Ellison[19] measured the electron affinity of CH_3SS via negative-ion photoelectron spectroscopy. Ma *et al.*[20] measured the photoionization efficiency of the methyl perthiyl radical in a supersonic beam and carried out *ab initio* calculations to explore possible isomerization on its ground state surface. Subsequent theoretical work by Cheung *et al.*[21] found several stable conformers of the methyl perthiyl radical with CH_3SS as the most stable. More recently, Maofa *et al.*[22] studied the ionization of CH_3SS using photoelectron spectroscopy and Martin-Diaconescu and Kennepohl[23] measured its X-ray absorption spectrum. While the above studies were concerned with the energetics and spectroscopy of the methyl perthiyl radical, none probed the specific photochemistry of the radical itself. The only previous study of perthiyl photodissociation was performed by Mikhailik *et al.* on the *tert*-butyl perthiyl radical in a hydrocarbon matrix at 365 nm.[24] Appearance of the *tert*-butyl radical was monitored using EPR, and the group concluded that the *tert*-butyl perthiyl radical was undergoing C–S bond fission to produce S_2 and the *tert*-butyl radical. The methyl perthiyl radical is of further interest as an isovalent analog to the methyl peroxy radical (CH_3OO), an important atmospheric and combustion intermediate.[25–27]

The ultraviolet absorption spectrum of CH_3SS has not been characterized. By analogy to CH_3O_2,[28] excitation at 248 nm may access the $\tilde{B}$ ($^2A''$) state of the radical.

[a] Current address: Agilent Technologies, 5301 Stevens Creek Blvd, Santa Clara, California 95051, USA.

[b] Author to whom correspondence should be addressed. Electronic mail: dneumark@berkeley.edu.

 © 2013 American Institute of Physics

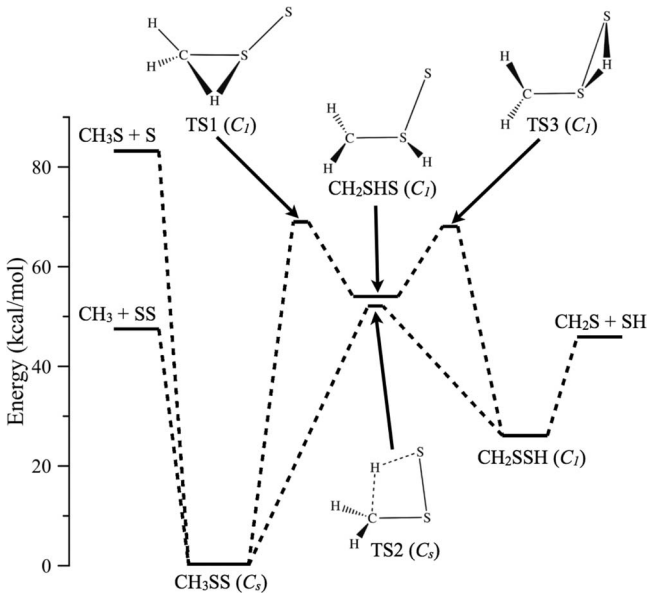

FIG. 1. Ground state potential energy surface for the isomerization and dissociation of the methyl perthiyl radical. Stationary points were calculated at the MP2(full)/6-31G(d) level of theory. Symmetries are given in parentheses. Exact structures can be found in Ref. 21.

At this wavelength, corresponding to a photon energy of 115 kcal/mol, there are several energetically allowed products from the photodissociation of the methyl perthiyl radical:

$$CH_3SS\,(\tilde{X}^2A'') + h\nu(248\,\text{nm}) \rightarrow CH_3\,(\tilde{X}^2A_2'') + SS\,(X^3\Sigma_g^-)$$
$$\Delta H_o = 47.5\,\text{kcal/mol}, \quad (3)$$

$$CH_3SS\,(\tilde{X}^2A'') + h\nu(248\,\text{nm}) \rightarrow CH_3S\,(\tilde{X}^2E) + S\,(^3P)$$
$$\Delta H_o = 83.2\,\text{kcal/mol}, \quad (4)$$

$$CH_3SS\,(\tilde{X}^2A'') + h\nu(248\,\text{nm}) \rightarrow CH_2S\,(\tilde{X}^1A_1) + SH\,(X^2\Pi)$$
$$\Delta H_o = 45.9\,\text{kcal/mol}, \quad (5)$$

Figure 1 shows asymptotic energetics and barrier heights for these channels on the ground state potential energy surface taken from previous experimental[15] and theoretical[21] work. On this surface, channels (3) and (4)[29] involve simple C–S or S–S bond fission, respectively, while channel (5)[21] requires isomerization prior to dissociation. As will be discussed in Sec. III, only channels (3) and (5) are observed in the 248 nm photodissociation of CH_3SS.

II. EXPERIMENTAL

A molecular beam of CH_3SS was produced by flash pyrolysis of DMDS and photodissociated; the photoproducts were mass-analyzed using a rotatable detector. Details about this instrument have been described elsewhere.[30,31] A piezoelectric valve produced a pulsed beam of 0.5% DMDS seeded in 2 atm of 10% N_2 in He. The N_2 was added to slow the molecular beam in order to facilitate detection of slower photofragments and to achieve better temporal separation of photofragments (see Sec. III). Methyl perthiyl radicals were generated using a resistively heated SiC flash pyrolysis source based on the design of Kohn *et al.*[32] and previously used by our laboratory to study the phenyl and *tert*-butyl radicals.[33,34] The radical beam was collimated by two skimmers that separate the source and main chambers of the machine. The beam was then crossed at 90° with the 248 nm output of a GAM EX100/500 excimer laser focused into a 3 × 1 mm^2 beam spot. Typical pulse energies were around 20 mJ/pulse. The laser and pulsed valve were operated at repetition rates of 100 Hz and 200 Hz, respectively, to allow for background subtraction. The scattered photofragments were detected as a function of laboratory scattering angle, Θ_{lab}, relative to the molecular beam in the plane defined by the molecular and laser beams. After entering the detector, photofragments were ionized by an electron impact ionizer, mass selected with a quadrupole mass filter, and detected with a Daly style ion detector.[35] Ion counts were recorded as a function of time relative to the laser pulse. The resulting time-of-flight (TOF) spectra were collected using a multichannel scaler interfaced to a computer. Typical TOF spectra were averaged over 100 000 to 200 000 laser shots. An iterative forward convolution program was used to simulate the TOF spectra for photoproducts over all angles, resulting in a photofragment translational energy distribution in the center-of-mass frame of reference.

The radical beam was characterized using a rotating, slotted chopper disk. Typical beam velocities were around 1500 m/s with speed ratios between 5 and 6. The beam was further characterized by taking mass spectra at $\Theta_{lab} = 0$ as the SiC tube temperature was increased. Intensities of the $CH_3SSCH_3^+$ ($m/z = 94$) and CH_3SS^+ ($m/z = 79$) signals were monitored as a function of current passing through the tube.

While complete removal of the precursor ion signal at $m/z = 94$ was possible, the remaining CH_3SS^+ signal at $m/z = 79$ was insubstantial under these very hot source conditions and the only photodissociation signal observed was $m/z = 32$ (S^+) from S_2 produced in the pyrolysis source; this signal was not observed under any other source conditions. As such, photodissociation data were taken under a variety of pyrolysis source conditions while monitoring the $m/z = 64$ photoproduct signal. Since $m/z = 64$, corresponding to the S_2 photoproduct, is not produced from the photodissociation of DMDS,[15] ion signal at this mass was assumed to be from the methyl perthiyl radical. This assumption was tested experimentally and will be discussed in Sec. IV. Because of incomplete precursor depletion from the beam and the large absorption cross section of dimethyl disulfide at 248 nm,[12] DMDS photodissociation experiments (pyrolysis source off) at 248 nm were also performed.

III. RESULTS

TOF spectra were taken for $m/z = 64$ (SS^+), $m/z = 47$ (CH_3S^+), $m/z = 46$ (CH_2S^+), $m/z = 45$ (CHS^+), $m/z = 33$ (SH^+), $m/z = 32$ (S^+), and $m/z = 15$ (CH_3^+), representing possible photofragments from channels (3)–(5) and daughter ions from dissociative ionization in the electron impact ionizer. Figure 2 shows sample TOF spectra for $m/z = 64$ at Θ_{lab}

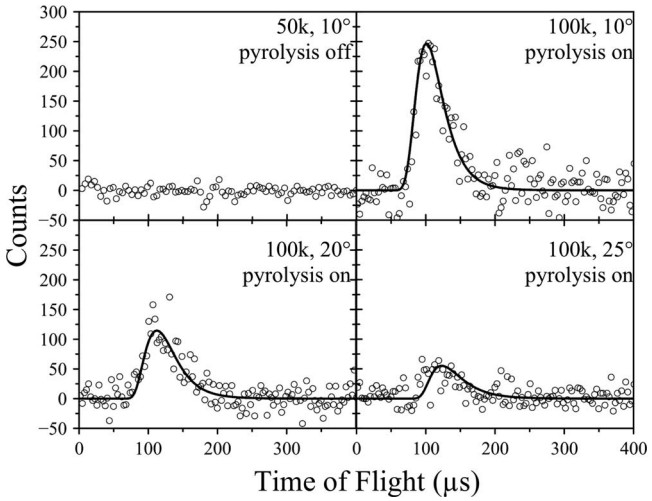

FIG. 2. Sample TOF spectra $m/z = 64$ (SS^+) collected at various Θ_{lab}. The top spectra show photodissociation signal without and with the pyrolysis source at $\Theta_{lab} = 10°$. The $P(E_T)$ shown in Fig. 4 was used to simulate the signal attributed to the methyl perthiyl radical (solid line). The number of laser shots averaged over is given in each TOF.

$= 10°$ with and without flash pyrolysis as well as spectra at selected larger scattering angles. Signal from $m/z = 64$ ions was seen over at laboratory angles as low as $\Theta_{lab} = 6°$ (the lowest angle spectrum recorded) and disappeared by $\Theta_{lab} = 30°$. These spectra were attributed to channel (3), an assignment discussed in Sec. IV. TOF data are represented by the open circles while the solid lines represent simulations obtained by forward convolution of a center-of-mass translational energy distribution (see Sec. IV). While we attempted to observe the corresponding CH_3 signal from radical photodissociation at $m/z = 15$, there was too much background from residual DMDS photodissociation to do so.

Evidence for a second channel can be observed in Fig. 3. At $\Theta_{lab} = 15°$, two peaks are resolved in the $m/z = 46$ and 45 TOF spectra but only one is seen at $m/z = 47$. The single peak at $m/z = 47$ and the larger, faster peaks at $m/z = 46$ and 45 are present up to $\Theta_{lab} = 30°$, the largest angle collected. The second, smaller peak is seen up to $\Theta_{lab} = 25°$. As discussed in more detail in Sec. IV, we attribute the slower peaks at $m/z = 46$ and 45 to the parent and daughter ion signals from the CH_2S photofragment produced via channel (5), while the faster peaks at these two masses and the single peak at $m/z = 47$ appear to be from DMDS photodissociation via channel (1). TOF spectra taken at $m/z = 33$ (SH^+) were inconclusive due to low signal levels, while $m/z = 32$ spectra were unusable due to contributions from DMDS photodissociation and high background gas signal.

IV. ANALYSIS

The results in Sec. III suggest that CH_3SS undergoes photodissociation via channels (3) and (5). In this section, we first analyze our data based on this assumption and then consider alternative interpretations. Center-of-mass photofragment translational and angular distributions, $P(E_T,\Theta)$ were obtained by simulating the TOF spectra of the photoproducts. For each channel, this distribution can be written as a product of uncoupled center-of-mass translational energy and angular distributions,

$$P(E_T, \Theta) = P(E_T)I(E_T, \Theta), \quad (6)$$

where $I(E_T,\Theta)$ is the angular distribution and $P(E_T)$ is the translational energy distribution. The PHOTRAN[36] forward convolution program was used to simulate all TOF spectra using assumed $P(E_T)$ distributions. The input $P(E_T)$ was adjusted point-wise until a satisfactory TOF simulation was achieved for all spectra. The experimental configuration used in this study has the detector rotating in the plane defined by the molecular and laser beams, so an anisotropic distribution is possible with unpolarized laser light. However, satisfactory agreement between simulation and experimental data was achieved by assuming isotropic distributions for all E_T. By conservation of energy, the total E_T available is given by

$$E_T = h\nu + E_o - E_{int} - D_o, \quad (7)$$

where $h\nu$ is the photon energy, E_o is the initial internal energy of the methyl perthiyl radicals, E_{int} is the internal energy of the photoproducts, and D_o is the bond dissociation energy. In the limit of cold radicals ($E_{int} = 0$), the maximum translational energy $E_{T,max}$ is given by $h\nu - D_o$. For channel (3), $E_{T,max} = 67.5$ kcal/mol whereas for channel (5), $E_{T,max} = 69.1$ kcal/mol.

The best TOF simulations for channels (3) and (5) are shown in Figures 4 and 5, respectively. The $P(E_T)$ distribution shown in Fig. 4, used to simulate channel (3), peaks at 6.1 kcal/mol and extends to 34 kcal/mol, 33.5 kcal/mol below the maximum allowable translational energy. The distribution has an average translational energy $\langle E_T \rangle = 10.4$ kcal/mol. The

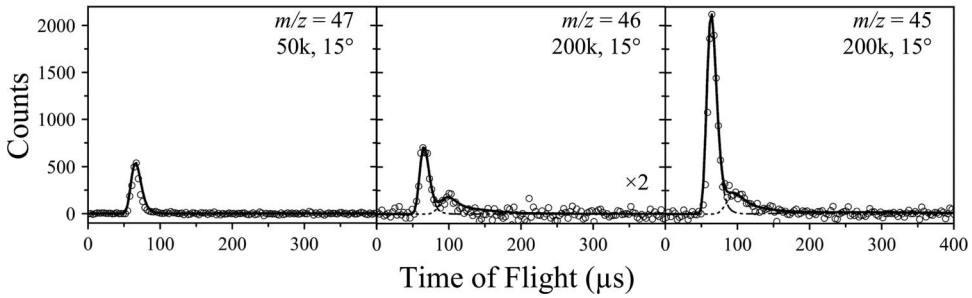

FIG. 3. TOF spectra showing evidence for channel (5). The fast, sharp peak appearing in all three spectra (dotted-dashed line) was well simulated as DMDS photodissociation using a $P(E_T)$ similar to that reported by Lee *et al.*[15] The second feature appearing in the $m/z = 46$ and 45 spectra was attributed to the CH_2S fragment from channel (5) and was simulated (dashed line) using the $P(E_T)$ in Fig. 5.

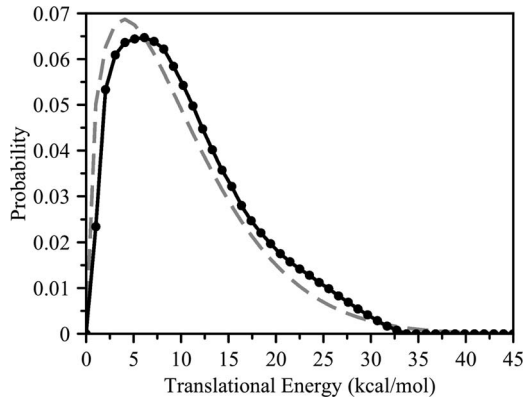

FIG. 4. Center-of-mass P(E_T) distribution for C–S fission (black curve). For this channel, $E_{T,\max} = 67.5$ kcal/mol. The prior distribution as described in Sec. V is also shown (dashed, grey curve).

P(E_T) distribution shown in Fig. 5 peaks at 5 kcal/mol and extends to 12 kcal/mol, which is 57.1 kcal/mol below the maximum allowable translational energy. This distribution has an average translational energy $\langle E_T \rangle = 5.8$ kcal/mol, implications of these P(E_T) distributions will be discussed in Sec. V.

The interpretation of our TOF data in terms of channels (3) and (5) is based on the observation of only a single fragment from each channel, rather than momentum-matched pairs of fragments as would be preferred when carrying out radical photodissociation experiments. Consideration must be given to sources of signal other than perthiyl photodissociation contributing to an observed TOF spectrum. In particular, owing to incomplete elimination of DMDS from the molecular beam, the 248 nm photodissociation of this species must be accounted for in all TOF spectra. As DMDS exclusively undergoes dissociation by channel (1) at 248 nm, the pyrolysis source-dependent peak at $m/z = 64$ is a strong indication of methyl perthiyl production and dissociation via channel (3).

The assignment of channel (5) is not as straightforward, especially in light of its best-fit P(E_T) distribution (see Sec. V). Dissociative ionization of CH_3S from DMDS channel (1) yields daughter ions in the $m/z = 46$ and 45 spectra in Fig. 3, partly obscuring the slower features. However, since the slower peaks in those spectra were not observed in the 248 nm photodissociation of DMDS (both in the present work and by Lee *et al.*[15]), these slower features are not from direct dissociation of the precursor. Another possibility is that this signal is from secondary photodissociation of CH_3S produced from DMDS via channel (1). While H-atom loss from CH_3S is energetically allowed at 248 nm,[37] the slower peaks in Fig. 3 were not observed in the DMDS photodissociation experiments where further photodissociation would have been obvious. Finally, it is possible that the signal in question could be from photodissociation of other DMDS pyrolysis products generated in the source, such as CH_3S or CH_2S. Attempts to simulate the signal as H + CH_2S from the photodissociation of CH_3S were unsuccessful. Trial P(E_T) functions ranged from low translational energy distributions similar to the work by Zheng *et al.*[38] to a distribution peaking at the maximum available translational energy of 67.5 kcal/mol. All of these yielded TOF simulations with photofragment arrival times later than the slower peak in the experimental spectra, particularly at larger laboratory angles. It thus appears that CH_3S photodissociation is an unlikely explanation for the slower feature in the $m/z = 46$ and 45 TOF spectra. If this signal were from CH_2S photodissociation, then there would only be signal at $m/z = 45$ and not $m/z = 46$. Overall, the slower peaks in Fig. 3 are most reasonably assigned to methyl perthiyl radical photodissociation via channel (5).

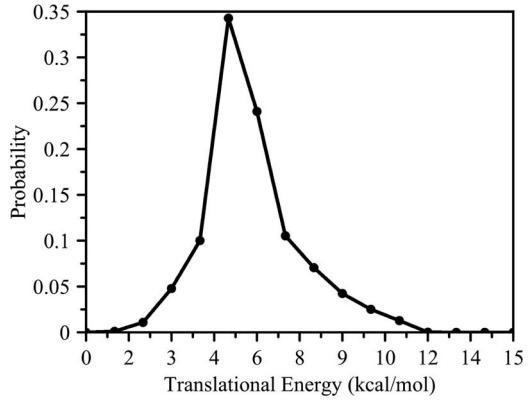

FIG. 5. Center-of-mass P(E_T) distribution for SH loss. For this channel, $E_{T,\max} = 69.1$ kcal/mol assuming ground state fragments.

V. DISCUSSION

The primary objectives of this study were (a) to probe the primary photochemistry of the methyl perthiyl radical and (b) to gain insight into the photodissociation mechanism at 248 nm. A key question is whether photodissociation occurs on an excited state surface or if the excited radical undergoes internal conversion to the ground state followed by statistical dissociation. This issue can be addressed by examining the translational energy distributions for the observed channels to see if they are consistent with statistical decay on the ground state surface.

Based on the schematic for the ground state surface in Fig. 1, no exit barriers are involved in the simple bond fission channels (3) and (4). In a statistical picture, the resulting P(E_T) distributions should be most intense at low translational energy with most of the energy distributed among the internal degrees of freedom. While channel (4) was not observed, channel (3) does peak at low translational energy, consistent with the high degree of internal excitation expected with ground state dissociation. To further test the hypothesis that channel (3) is statistical, a prior distribution was calculated using the functional form[39]

$$\mathrm{P}(E_T|E_{\mathrm{avail}}) \propto E_T^{1/2} \rho_{\mathrm{vr}}(E_{\mathrm{avail}} - E_T), \tag{8}$$

where E_T is the translational energy and $\rho_{\mathrm{vr}}(E_{\mathrm{avail}} - E_T)$ is the rotational-vibrational density of states for the pair of fragments. To implement Eq. (8) for channel (3), five total rotational degrees of freedom and seven total vibrational degrees of freedom (treated as classical harmonic oscillators) were used. The resulting prior distribution for channel (3), shown in Fig. 4 as the dashed grey line, agrees reasonably well with the experimentally derived P(E_T), suggesting that dissociation for this channel occurs statistically on the ground state surface.

The P(E_T) distribution for channel (5) falls off more rapidly as $E_T \rightarrow 0$ than the distribution for channel (3), a result suggesting ground state dissociation over a small exit barrier. Such a result can be rationalized with reference to Fig. 1, which shows that the lower energy pathway to channel (3) involves isomerization over TS2 and then passage through a shallow well (19.8 kcal/mol with respect to products) corresponding to the CH_2SSH structure. Under these circumstances, energy randomization in this well may not occur, with the overall P(E_T) distribution still reflecting the effect of TS2. However, the form of this distribution is still unusual, as it implies a significant degree of product internal energy confined within a narrow range of only a few kcal/mol. It is possible that this signal corresponds to CH_2S in its first electronic excited state ($\tilde{A}\ ^1A_2$), which lies only 47 kcal/mol[40] above the thioformaldehyde ground state with a corresponding $E_{T,\max}$ of 22 kcal/mol. Full elucidation of the dissociation mechanism requires more information than is presently available. Observation of the SH photofragment and a determination of the translational energy (or internal energy distribution via techniques such as laser induced fluorescence) would provide further insight into the exact dynamical process. Calculation of the excited state potential energy surfaces for CH_3SS would also provide valuable insight.

The results for the methyl perthiyl radical can be compared to the 248 nm photofragmentation of the methyl peroxy (CH_3O_2) radical by Hartmann *et al.*[41] In that experiment, ground state OH and CH_3O products were seen by laser-induced fluorescence, and emission from electronically excited OH($A^2\Sigma^+$) was also observed. These are the analogues to channels (4) and (5) in CH_3SS photodissociation. Although Hartmann *et al.* were not set up to detect $CH_3 + O_2$ products, the analogue to channel (3), they proposed, based on quantum yield measurements, that this was in fact the dominant channel (74%), followed by $CH_3O + O$ (20%) and $CH_2O + OH$ (6%). However, the asymptotic energetics for CH_3O_2 dissociation are very different than for CH_3SS; the lowest energy channel is production of $CH_2O + OH$, which lies 21 kcal/mol below CH_3O_2, 52 kcal/mol below $CH_3 + O_2$ and 80 kcal/mol below $CH_3O + O$. The observation of OH($A^2\Sigma^+$) indicates that at least some dissociation of CH_3O_2 occurs on an excited state surface. Direct characterization of the $CH_3 + O_2$ channel would be of considerable interest to see if that channel is indeed dominant and if so, whether its dynamics are consistent with ground state dissociation.

VI. CONCLUSIONS

The photodissociation dynamics of the methyl perthiyl radical has been explored at 248 nm using photofragment translational spectroscopy. Two channels were observed, $CH_3 + SS$ and $CH_2S + SH$. The translational energy distribution for channel (3), $CH_3 + SS$, is similar to that expected for a simple statistical distribution, suggesting that the methyl perthiyl radical undergoes internal conversion to the ground state prior to dissociation to these products. Channel (5), $CH_2S + SH$, can occur via isomerization on the ground state surface but could also involve production of electronically excited CH_2S.

ACKNOWLEDGMENTS

This work was supported by the Director, Office of Basic Energy Sciences, Chemical Sciences, Geosciences, and Biosciences Division of the U.S. Department of Energy under Contract No. DE-AC02-05CH11231.

[1] R. J. Huxtable and W. M. Lafranconi, *Biochemistry of Sulfur* (Plenum, 1986).
[2] T. E. Graedel, Rev. Geophys. **15**, 421, doi:10.1029/RG015i004p00421 (1977).
[3] P. M. Rao, J. A. Copeck, and A. R. Knight, Can. J. Chem. **45**, 1369 (1967).
[4] A. B. Callear and D. R. Dickson, Trans. Faraday Soc. **66**, 1987 (1970).
[5] G. W. Byers, H. N. Schott, H. G. Giles, J. A. Kampmeier, and H. Gruen, J. Am. Chem. Soc. **94**, 1016 (1972).
[6] K. Ohbayashi, H. Akimoto, and I. Tanaka, Chem. Phys. Lett. **52**, 47 (1977).
[7] R. J. Balla and J. Heicklen, Can. J. Chem. **62**, 162 (1984).
[8] M. Suzuki, G. Inoue, and H. Akimoto, J. Chem. Phys. **81**, 5405 (1984).
[9] R. J. Balla and J. Heicklen, J. Photochem. **29**, 297 (1985).
[10] T. J. Burkey, J. A. Hawari, F. P. Lossing, J. Lusztyk, R. Sutcliffe, and D. Griller, J. Org. Chem. **50**, 4966 (1985).
[11] R. J. Balla, H. H. Nelson, and J. R. McDonald, Chem. Phys. **109**, 101 (1986).
[12] G. Black and L. E. Jusinski, Chem. Phys. Lett. **131**, 310 (1986).
[13] G. Black and L. E. Jusinski, J. Chem. Soc., Faraday Trans. 2 **82**, 2143 (1986).
[14] S. Nourbakhsh, C. L. Liao, and C. Y. Ng, J. Chem. Phys. **92**, 6587 (1990).
[15] Y. R. Lee, C. L. Chiu, and S. M. Lin, J. Chem. Phys. **100**, 7376 (1994).
[16] B. Martínez-Haya, M. J. Bass, M. Brouard, C. Vallance, I. Torres, and J. Barr, J. Chem. Phys. **120**, 11042 (2004).
[17] A. Rinker, C. D. Halleman, and M. R. Wedlock, Chem. Phys. Lett. **414**, 505 (2005).
[18] A. Kumar, P. K. Chowdhury, K. Rao, and J. P. Mittal, Chem. Phys. Lett. **198**, 406 (1992).
[19] S. Moran and G. B. Ellison, J. Phys. Chem. **92**, 1794 (1988).
[20] Z. X. Ma, C. L. Liao, C. Y. Ng, Y. S. Cheung, W. K. Li, and T. Baer, J. Chem. Phys. **100**, 4870 (1994).
[21] Y. S. Cheung, W. K. Li, and C. Y. Ng, J. Mol. Struct.: THEOCHEM **339**, 25 (1995).
[22] G. Maofa, W. Jing, S. Zheng, Z. Xinjiang, and W. Dianxun, J. Chem. Phys. **114**, 3051 (2001).
[23] V. Martin-Diaconescu and P. Kennepohl, J. Am. Chem. Soc. **129**, 3034 (2007).
[24] V. V. Mikhailik, Y. V. Razskazovskii, and M. Y. Mel'nikov, Dokl. Akad. Nauk **263**, 934 (1982).
[25] P. D. Lightfoot, R. A. Cox, J. N. Crowley, M. Destriau, G. D. Hayman, M. E. Jenkin, G. K. Moortgat, and F. Zabel, Atmos. Environ., Part A **26**, 1805 (1992).
[26] G. J. Frost, G. B. Ellison, and V. Vaida, J. Phys. Chem. A **103**, 10169 (1999).
[27] C. A. Taatjes, J. Phys. Chem. A **110**, 4299 (2006).
[28] T. J. Wallington, P. Dagaut, and M. J. Kurylo, Chem. Rev. **92**, 667 (1992).
[29] S. W. Benson, Chem. Rev. **78**, 23 (1978).
[30] Y.-T. Lee, J. D. McDonald, P. R. LeBreton, and D. R. Herschbach, Rev. Sci. Instrum. **40**, 1402 (1969).
[31] J. C. Robinson, S. A. Harris, W. Sun, N. E. Sveum, and D. M. Neumark, J. Am. Chem. Soc. **124**, 10211 (2002).
[32] D. W. Kohn, H. Clauberg, and P. Chen, Rev. Sci. Instrum. **63**, 4003 (1992).
[33] B. Negru, S. J. Goncher, A. L. Brunsvold, G. M. P. Just, D. Park, and D. M. Neumark, J. Chem. Phys. **133**, 074302 (2010).
[34] B. Negru, G. M. P. Just, D. Park, and D. M. Neumark, Phys. Chem. Chem. Phys. **13**, 8180 (2011).
[35] N. R. Daly, Rev. Sci. Instrum. **31**, 264 (1960).
[36] S. A. Harich, PHOTRAN, 2003.
[37] C.-W. Hsu, C.-L. Liao, Z.-X. Ma, P. J. H. Tjossem, and C. Y. Ng, J. Chem. Phys. **97**, 6283 (1992).
[38] X. Zheng, Y. Song, J. Wu, and J. Zhang, Chem. Phys. Lett. **467**, 46 (2008).
[39] T. Baer and W. L. Hase, *Unimolecular Reaction Dynamics: Theory and Experiments* (Oxford University Press, 1996).
[40] R. H. Judge and G. W. King, J. Mol. Spectrosc. **74**, 175 (1979).
[41] D. Hartmann, J. Karthaeuser, and R. Zellner, J. Phys. Chem. **94**, 2963 (1990).